
Does Confidence Calibration Help Conformal Prediction?

Huajun Xi^{*1} Jianguo Huang^{*2} Lei Feng³ Hongxin Wei¹

Abstract

Conformal prediction, as an emerging uncertainty qualification technique, constructs prediction sets that are guaranteed to contain the true label with high probability. Previous works usually employ temperature scaling to calibrate the classifier, assuming that confidence calibration can benefit conformal prediction. In this work, we first show that post-hoc calibration methods surprisingly lead to larger prediction sets with improved calibration, while over-confidence with small temperatures benefits the conformal prediction performance instead. Theoretically, we prove that high confidence reduces the probability of appending a new class in the prediction set. Inspired by the analysis, we propose a novel method, **Conformal Temperature Scaling** (ConfTS), which rectifies the objective through the gap between the threshold and the non-conformity score of the ground-truth label. In this way, the new objective of ConfTS will optimize the temperature value toward an optimal set that satisfies the *marginal coverage*. Experiments demonstrate that our method can effectively improve widely-used conformal prediction methods.

1. Introduction

Ensuring the reliability of model predictions is crucial for the safe deployment of machine learning applications. Numerous methods have been developed to estimate and incorporate uncertainty into predictive models, including confidence calibration (Guo et al., 2017), MC-Dropout (Gal & Ghahramani, 2016), and Bayesian neural network (Smith, 2013). *Conformal prediction* (CP), on the other hand, offers a systematic approach to constructing prediction sets that contain ground-truth labels with a predefined coverage

guarantee (Vovk et al., 2005; Shafer & Vovk, 2008; Balasubramanian et al., 2014; Angelopoulos & Bates, 2021). This framework provides transparency and trustworthiness in real-world applications where wrong predictions can be costly and dangerous.

In the literature, conformal prediction is frequently associated with *confidence calibration*, which expects the predicted class probability to represent the true correctness likelihood (Yuksekgonul et al., 2023; Wei et al., 2022; Wang et al., 2021). For example, existing CP methods usually utilize temperature scaling (Guo et al., 2017) to process the model output for a better calibration performance (Angelopoulos et al., 2021b; Lu et al., 2022; 2023; Gibbs et al., 2023). The underlying hypothesis is that well-calibrated models yield precise probability estimates, thereby enhancing the reliability of prediction sets. Yet, the influence of calibration on conformal prediction remains ambiguous. This motivates our thorough analysis of the connection between conformal prediction and confidence calibration.

In this paper, we empirically show that post-hoc calibration methods increase the size of the prediction set, while improving calibration performance. More surprisingly, over-confident models often result in compact prediction sets, while holding coverage rate. Theoretically, we prove that using a small temperature will reduce the probability of appending a new class in the prediction set. However, simply adopting an extremely small temperature makes it challenging to generate meaningful prediction sets and maintain the coverage rate. Thus, we aim to design a calibration method that aligns with the objective of conformal prediction.

To this end, we propose a novel method, *Conformal Temperature Scaling* (ConfTS), which rectifies the objective of temperature scaling with the compactness gap, i.e., the gap between the threshold and the non-conformity score of the ground-truth label. Specifically, we optimize the compactness gap to maintain the coverage rate with the corresponding positive probability. In effect, our ConfTS method encourages the positive probability of the compactness gap to be consistent with the coverage rate. Calibrated with ConfTS, the prediction set can be optimized to be compact while maintaining the property of marginal coverage.

Extensive experiments demonstrate the effectiveness of ConfTS over existing methods for conformal prediction. First,

^{*}Equal contribution ¹Department of Statistics and Data Science, Southern University of Science and Technology ²The School of Information Science and Technology, ShanghaiTech University ³School of Computer Science and Engineering, Nanyang Technological University. Correspondence to: Hongxin Wei <weihx@sustech.edu.cn>.

our method drastically improves the compactness of the prediction sets produced by APS (Romano et al., 2020) and RAPS (Angelopoulos et al., 2021b). For example, using the ImageNet dataset, ConfTr reduces the set size of APS with $\alpha = 0.1$ from 10.9 to 3.91 – an improvement of 6.99 over the vanilla models. Moreover, we show that our method also maintains the adaptiveness of APS and RAPS: larger sets for challenging samples and narrower sets for easier samples.

Overall, using *Conformal Temperature scaling* decreases the set size in conformal prediction while maintaining a valid coverage rate. Additionally, the computation of ConfTS does not require hyperparameter tuning and extra computation cost. It is straightforward to implement with existing trained models.

We summarize our contributions as follows:

1. We empirically show that calibrated models typically lead to larger prediction sets. Conversely, highly confident models always lead to efficient prediction sets.
2. We provide theoretical analysis in Proposition 3.1 and Theorem 3.2 to demonstrate that a small temperature can lead to a low probability of appending a new class in the prediction set.
3. We propose ConfTS – a simple and effective post-hoc method to decrease the set size while maintaining the marginal coverage guarantee. The key idea is to minimize the distance between the desired coverage rate and the positive probability of the compactness gap.

2. Preliminary

In this work, we consider the multi-class classification task with K classes. Let $\mathcal{X} \subset \mathbb{R}^d$ be the input space and $\mathcal{Y} := \{1, \dots, K\}$ be the label space. We use $\hat{\pi} : \mathcal{X} \rightarrow \mathbb{R}^K$ to denote the pre-trained neural network that is used to predict the label of a test instance. Let $(X, Y) \sim \mathcal{P}_{\mathcal{X}\mathcal{Y}}$ denote a random data pair satisfying a joint data distribution $\mathcal{P}_{\mathcal{X}\mathcal{Y}}$ and $\mathbf{f}_y(\mathbf{x})$ denotes the y -th element of logits vector $\mathbf{f}(\mathbf{x})$ corresponding to the ground-truth label y . The conditional probability of class y can be approximated by softmax probability $\pi_y(\mathbf{x})$, where

$$\pi_y(\mathbf{x}) = \sigma(\mathbf{f}(\mathbf{x}))_y = \frac{e^{\mathbf{f}_y(\mathbf{x})}}{\sum_{i=1}^K e^{\mathbf{f}_i(\mathbf{x})}}.$$

where σ is a softmax function. Let the softmax probability distribution be

$$\boldsymbol{\pi}(\mathbf{x}) = (\pi_1(\mathbf{x}), \pi_2(\mathbf{x}), \dots, \pi_K(\mathbf{x}))$$

Then, the classification prediction is given by $\hat{y} = \operatorname{argmax}_{y \in \mathcal{Y}} \pi_y(\mathbf{x})$.

Conformal prediction. To provide a formal guarantee for the model performance, conformal prediction (Vovk et al., 2005) is designed to produce prediction sets containing ground-truth labels with a desired probability. Instead of predicting one-hot labels from the model outputs, the goal of conformal prediction is to construct a set-valued mapping $\mathcal{C} : \mathcal{X} \rightarrow 2^{\mathcal{Y}}$, which satisfies the *marginal coverage*:

$$\mathbb{P}(Y \in \mathcal{C}(X)) \geq 1 - \alpha, \quad (1)$$

where $\alpha \in (0, 1)$ denotes the desired error rate and $\mathcal{C}(X)$ is a subset of \mathcal{Y} .

Before deployment, conformal prediction begins with a calibration step, using a calibration set $\mathcal{D}_{cal} := \{(\mathbf{x}_i, y_i)\}_{i=1}^n$. The examples of the calibration set are also i.i.d. drawn from the distribution $\mathcal{P}_{\mathcal{X}\mathcal{Y}}$. Specifically, we calculate a non-conformity score $s_i = S(\mathbf{x}_i, y_i)$ for each example (\mathbf{x}_i, y_i) in the calibration set, where s_i measures the degree of deviation between the given example and the training data. The $1 - \alpha$ quantile of the non-conformity scores $\{s_i\}_{i=1}^n$ is then determined as a threshold τ . Formally, the value of τ can be obtained as shown below:

$$\tau = \inf \left\{ s : \frac{|\{i \in \{1, \dots, n\} : s_i \leq s\}|}{n} \geq \frac{\lceil (n+1)(1-\alpha) \rceil}{n} \right\}. \quad (2)$$

During testing, we calculate the non-conformity score for each label given a new instance \mathbf{x}_{n+1} . Then, the corresponding prediction set $\mathcal{C}(\mathbf{x}_{n+1})$ comprises possible labels whose non-conformity score $S(\mathbf{x}_{n+1}, y)$ falls within $\hat{\tau}$:

$$\mathcal{C}(\mathbf{x}_{n+1}) = \{y \in \mathcal{Y} : S(\mathbf{x}_{n+1}, y) \leq \tau\}. \quad (3)$$

Adaptive Prediction Set (APS) In the APS method (Romano et al., 2020), the non-conformity scores are calculated by accumulating sorted softmax probabilities:

$$S(\mathbf{x}, y) = \pi_{(1)}(\mathbf{x}) + \dots + \pi_{o(y, \boldsymbol{\pi}(\mathbf{x}))}(\mathbf{x}), \quad (4)$$

where $\pi_{(1)}(\mathbf{x}), \pi_{(2)}(\mathbf{x}), \dots, \pi_{(k)}(\mathbf{x})$ are the sorted softmax probabilities in descending order, $o(y, \boldsymbol{\pi}(\mathbf{x}))$ represents the order of $\pi_y(\mathbf{x})$.

Regularized Adaptive Prediction Set (RAPS) The conformity scoring function of regularized APS (Angelopoulos et al., 2021b), i.e., RAPS, encourages small set size by adding a penalty to classes. Formally, the score function is defined as:

$$S(\mathbf{x}, y) = \pi_{(1)}(\mathbf{x}) + \dots + \pi_{o(y, \boldsymbol{\pi}(\mathbf{x}))}(\mathbf{x}) + \lambda \cdot (o(y, \boldsymbol{\pi}(\mathbf{x})) - k_{reg})^+, \quad (5)$$

where $(z)^+ = \max\{0, z\}$ and k_{reg} is to control the number of penalized classes.

can show that the prediction sets satisfy the coverage property defined in Eq. 1, as shown in the following theorem.

Table 1. Prediction set performance with different calibration methods: baseline (BS), i.e., no calibration method, vector scaling (VS), Platt scaling (PS), and temperature scaling (TS). We employ three models: ResNet18, ResNet50, and ResNet101 on CIFAR100 and Imagenet. We report the mean value over 10 trials. ↓ indicates smaller values are better.

Datasets	Metrics	ResNet18				ResNet50				ResNet101				
		BS	VS	PS	TS	BS	VS	PS	TS	BS	VS	PS	TS	
CIFAR100	Accuracy	0.76	0.75	0.76	0.76	0.77	0.77	0.77	0.77	0.78	0.79	0.78	0.78	
	ECE(%) ↓	5.68	3.67	4.2	4.29	8.79	3.62	3.81	4.06	10.87	3.27	3.83	3.62	
	APS	Coverage	0.9	0.89	0.9	0.9	0.9	0.9	0.9	0.9	0.9	0.89	0.9	0.9
		Average size ↓	8.73	8.16	9.73	9.77	4.91	6.09	7.36	7.25	4.01	5.6	6.57	6.78
	RAPS	Coverage	0.9	0.89	0.9	0.9	0.9	0.9	0.9	0.9	0.9	0.89	0.9	0.9
		Average size ↓	7.23	6.88	8.4	8.48	4.16	5.15	6.41	6.29	3.32	4.86	5.83	5.66
ImageNet	Accuracy	0.69	0.68	0.69	0.69	0.76	0.75	0.76	0.76	0.77	0.76	0.77	0.77	
	ECE(%) ↓	2.63	2.14	2.1	2.27	3.69	1.5	2.24	2.35	5.08	1.38	2.02	2.2	
	APS	Coverage	0.9	0.88	0.9	0.9	0.9	0.88	0.9	0.9	0.9	0.88	0.9	0.9
		Average size ↓	14.13	12.9	15.41	15.93	9.06	8.89	11.76	12.74	6.95	8.27	11.04	10.65
	RAPS	Coverage	0.9	0.88	0.9	0.9	0.9	0.88	0.9	0.9	0.9	0.88	0.9	0.9
		Average size ↓	9.33	9.22	10.91	11.14	6.1	6.27	7.93	7.87	4.77	5.62	7.07	7.93

Theorem 2.1. (Vovk et al., 1999) Suppose $(\mathbf{x}_i, y_i)_{i=1}^n$ and $(\mathbf{x}_{\text{test}}, y_{\text{test}})$ are exchangeable data samples. Defining τ as:

$$\tau = \inf \left\{ s : \frac{|\{i : \mathcal{S}(\mathbf{x}_i, y_i) \leq s\}|}{n} \geq \frac{[(n+1)(1-\alpha)]}{n} \right\}$$

and the resulting prediction sets as:

$$\mathcal{C}(\mathbf{x}) = \{y : \mathcal{S}(\mathbf{x}, y) \leq \tau\}.$$

Then,

$$\mathbb{P}\{Y_{\text{test}} \in \mathcal{C}(\mathbf{x}_{\text{test}})\} \geq 1 - \alpha.$$

In practice, we use *coverage* and *inefficiency* to evaluate the prediction set. *Coverage* measures the percentage of samples whose prediction sets contain true labels:

$$\text{Coverage} = \frac{1}{|\mathcal{I}_{\text{test}}|} \sum_{i \in \mathcal{I}_{\text{test}}} \mathbf{1}\{y_i \in \mathcal{C}(\mathbf{x}_i)\} \quad (6)$$

where $\mathbf{1}$ is the indicator function. Average size (or inefficiency) is a measurement for the compactness of prediction sets:

$$\text{Average size} = \frac{1}{|\mathcal{I}_{\text{test}}|} \sum_{i \in \mathcal{I}_{\text{test}}} |\mathcal{C}(\mathbf{x}_i)| \quad (7)$$

The prediction sets should both provide the desired coverage rate and compactness (i.e., small prediction sets). Compact prediction sets are preferred, as they convey more detailed information, being meaningful for practical decision (Angelopoulos et al., 2021b).

3. Motivation

3.1. Conformal prediction with calibrated models

Model calibration (Wang, 2023; Guo et al., 2017; Mukhoti et al., 2020; Müller et al., 2019) expects the neural networks to predict softmax probabilities, which can faithfully estimate the true probabilities of correctness. Formally, a *perfectly* calibrated model satisfies:

$$\hat{\pi}_y(\mathbf{x}) = \pi_y(\mathbf{x})$$

where $\pi_y(\mathbf{x})$ and $\hat{\pi}(\mathbf{x})$ are the true and estimated probability distribution defined in Section 2. To qualify the degree of miscalibration, the *Expected Calibration Error* (ECE) is defined as the difference between the accuracy and confidence. In particular, it partitions predictions into M equally-spaced bins and takes a weighted average of the bins’ accuracy/confidence difference. Formally,

$$\text{ECE} = \sum_{m=1}^M \frac{|B_m|}{|\mathcal{I}_{\text{test}}|} |\text{acc}(B_m) - \text{conf}(B_m)| \quad (8)$$

where $\text{acc}(\cdot)$ and $\text{conf}(\cdot)$ denotes the average accuracy and confidence in bin B_m .

Previous works on conformal prediction typically assume that model calibration positively impacts prediction sets, thus applying temperature scaling to calibrate neural models (Angelopoulos et al., 2021b; Lu et al., 2022; 2023; Gibbs et al., 2023). However, the effect of the calibration methods on conformal prediction remains unexplored. In this section,

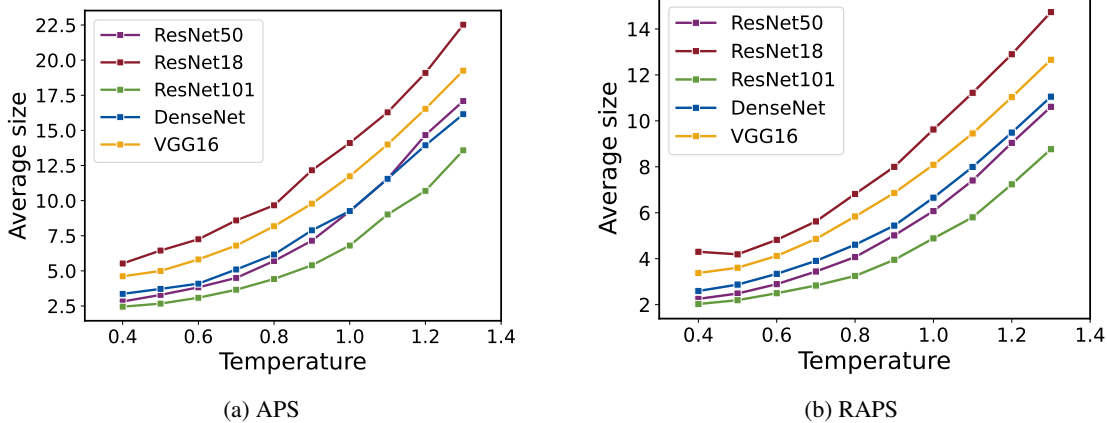


Figure 1. Performance comparison of conformal prediction with various temperatures. We report the average set size of APS and RAPS using five pre-trained models on ImageNet.

we analyze how various model calibration methods affect the average size and coverage rate of prediction sets. In particular, we consider a variety of popular post-hoc calibration methods, i.e., vector scaling (Guo et al., 2017), Platt scaling (Platt et al., 1999), and temperature scaling (Guo et al., 2017), which are detailed introduced in Appendix A. The detailed experiment setup and supplementary experiment results are provided in Appendix B and Appendix D.

How does model calibration affect conformal prediction?

Table 1 demonstrates that models calibrated by various methods tend to generate larger prediction sets, i.e., worse performance in compactness. For example, on CIFAR-100, the original average size of ResNet50 with respect to APS is 4.91 but increases to 6.09 with vector scaling, 7.36 with Platt scaling, and 7.25 with temperature scaling. We intuitively explain this phenomenon: the calibrated model tends to be conservative in its predictions, thereby generating large prediction sets to exhibit high uncertainty. Moreover, we analyze the coverage rate in Appendix C.

Overall, empirical results demonstrate that calibrated models typically yield larger prediction sets, which might conflict with the goal of conformal prediction. This fact challenges the prevalent belief that model calibration can enhance the performance of conformal prediction. This motivates us to explore the optimal confidence level for conformal prediction.

3.2. Conformal prediction with over-confident models

The above section demonstrates that APS and RAPS construct larger prediction sets with post-hoc calibration methods. In this section, we further investigate how the confidence level impacts the conformal prediction. In the analysis, we compare the compactness of prediction sets generated by models with various temperatures

$\{0.4, 0.5, \dots, 1.3\}$. The detailed experiment setup and supplementary experiment results are provided in Appendix B and Appendix D.

High confidence promotes a compact prediction set.

In Figure 1, we observe that, overconfident models, i.e., models with small temperature values, can generate small prediction sets for both APS and RAPS. These observations align with our previous hypothesis: a confident prediction can yield a compact prediction set with less uncertainty. In addition, the coverage rate is provided in appendix D, which shows that the coverage rate of APS and RAPS stabilizes at about 0.9. Note that RAPS produces a relatively large set with a minimal temperature, we will analyze the negative effect of small temperatures in the latter (See Figure 2).

To summarize, high-confidence predictions can yield compact prediction sets, being informative in practical applications. In the above analysis, we show that the confidence level can significantly impact prediction sets. we proceed by a formal analysis to explain this phenomenon.

3.3. Theoretical explanation

In this section, we provide a formal justification for the above phenomenon in the case of APS. Our main Theorem 3.2 gives a provable understanding of how the temperature reduces the average size of prediction sets. All the omitted proofs are presented in Appendix E. To start with, we analyze how the non-conformity score of APS correlates with the temperature. Note that we have defined the score in eq 4. Here, for simplicity, assume the logits vector \mathbf{f} follows $f_1 > f_2 > \dots > f_K$. We can rewrite the score by

$$\mathcal{S}(\mathbf{x}, y, t) = \sum_{i=1}^k \frac{e^{f_i/t}}{\sum_{j=1}^K e^{f_j/t}} \quad (9)$$

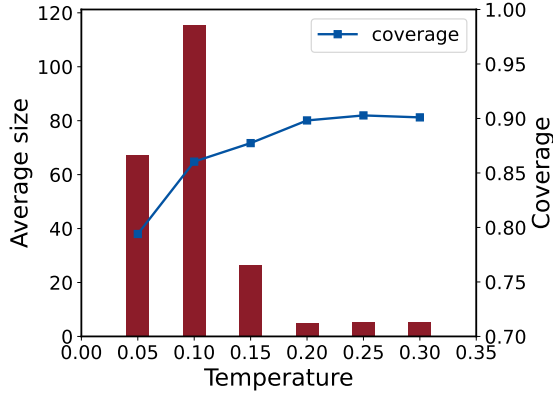


Figure 2. Analysis of conformal prediction with small temperatures. We report the average size and coverage rate of APS using the ResNet18 model on ImageNet.

Then, we can have the following proposition:

Proposition 3.1. *For any data sample (\mathbf{x}, y) , let $\mathcal{S}(\mathbf{x}, y, t)$ denote the non-conformity scores. If $t_1 \geq t_2$, we have*

$$\mathcal{S}(\mathbf{x}, y, t_1) \leq \mathcal{S}(\mathbf{x}, y, t_2)$$

This proposition shows that as the temperature reduces, the sample will obtain an increased non-conformity score. We then have the following theorem to explain why the average size of prediction sets diminishes with the increased scores.

Theorem 3.2. *Given a well-calibrated model, for any data sample \mathbf{x} , let its non-conformity score be $\mathcal{S}(\mathbf{x}, y)$, threshold be τ and has prediction set \mathcal{C} ; after applying temperature $t < 1$, let its non-conformity score be $\mathcal{S}'(\mathbf{x}, y)$, threshold be τ' , and has prediction set \mathcal{C}' . Let $G_y(\cdot)$ denote the CDF of $\mathcal{S}(\mathbf{x}, y)$. Give the assumption that*

- (a) $\mathbb{P}\{\sup_{\mathbf{x}}\{\mathcal{S}'(\mathbf{x}, y) - \mathcal{S}(\mathbf{x}, y)\} \leq \epsilon\} \leq \delta$
- (b) $\exists \gamma, c_1, c_2, \epsilon_0, \forall \epsilon \in [-\epsilon_0, \epsilon_0]$
s.t. $c_1|\epsilon|^\gamma \leq |G_y(t + \epsilon) - G_y(t)| \leq c_2|\epsilon|^\gamma$

Then, there exists a constant c such that with probability $1 - K\delta - n^{-1}$:

$$\mathbb{P}\{y \in \mathcal{C}/\mathcal{C}'\} \geq 2\epsilon + \{(K + 1)cc_1^{-1}(\log n/n)\}^{1/\gamma}$$

Remark 3.3. In the theorem, we make two assumptions: the first assumption depicts how \mathcal{S}' increases with temperature. The second assumption is on the density of $G_y(\cdot)$ near the cut-off value. Here we use $\mathbb{P}\{y \in \mathcal{C}/\mathcal{C}'\}$ (the probability of y is contained in origin prediction set \mathcal{C} but not contained in \mathcal{C}' after employed with a temperature $t < 1$). A similar analysis is also used in previous work (Lei, 2014; Sadinle et al., 2019), which analyzes $\mathbb{P}\{y \in \mathcal{C}/\mathcal{C}'\}$ to mirror how prediction sets perform with plug-in methods that asymptotically mimic the optimal procedures.

In this analysis, we use ϵ to denote the increment of the non-conformity score. To explain the reduction of average size, we show that the probability that the prediction set will narrow, i.e. $\mathbb{P}\{y \in \mathcal{C}/\mathcal{C}'\}$, increases. Essentially, $\mathbb{P}\{y \in \mathcal{C}/\mathcal{C}'\}$ measures the likelihood that an arbitrary class y originally in the prediction set \mathcal{C} but not in the new set \mathcal{C}' , and thus higher probability indicates reduced average size. Theorem 3.2 states that under the mild assumption, this likelihood is lower bound by $\epsilon + \text{const}$. This implies that as the non-conformity score increases, the prediction set becomes less likely to append a new class.

However, in practice, an exceedingly low temperature can pose challenges for prediction sets. We illustrate the performance of APS under low temperatures in Figure 2, using the ResNet18 model. We can observe that after employing a small temperature, the prediction set may become larger and struggle to achieve the desired coverage rate. In light of this phenomenon, it is imperative to devise a novel loss function that facilitates the achievement of an appropriate temperature.

4. Method: Conformal Temperature Scaling

In the previous analysis, we demonstrated that the temperature optimized with cross-entropy loss often deteriorates the performance of conformal prediction. In this section, we propose to design a new loss function for temperature scaling, to align with the objective of conformal prediction.

For a given instance (\mathbf{x}, y) , conformal prediction aims to construct a compact prediction set $\mathcal{C}(\mathbf{x})$ that contains the ground-truth label y . Thus, we define the optimal prediction set as:

$$\mathcal{C}^*(\mathbf{x}) = \{\hat{y} \in \mathcal{Y} : \mathcal{S}(\mathbf{x}, \hat{y}) \leq \mathcal{S}(\mathbf{x}, y)\},$$

Specifically, the optimal prediction set is with the smallest size that allows the inclusion of the ground-true label. To evaluate the compactness of a given prediction set \mathcal{C} , a natural idea is to calculate the difference between the size of the prediction set and the optimal prediction set: $(|\mathcal{C}| - |\mathcal{C}^*|)$. Yet, it is challenging to conduct optimization with the objective of the size difference due to its discrete property. To circumvent the issue, we convert the objective into a continuous loss function that can be end-to-end trainable.

Compactness gap. Recall that the prediction set is established through the τ calculated from the calibration set (Eq. 2), the optimal set can be attained if the threshold τ well approximates the non-conformity score of the ground-truth label $\mathcal{S}(\mathbf{x}, y)$. Therefore, we can also measure the compactness of the prediction set by the differences between thresholds τ and the score of true labels, defined as:

Definition 4.1 (Compactness Gap). For an arbitrary sample

Table 2. Performance comparison of different non-conformity scores with or without ConfTS on ImageNet dataset. \downarrow indicates smaller values are better. **Bold** numbers are superior results.

Model	Conformal	alpha=0.1		alpha=0.05	
		Coverage	Average size \downarrow	Coverage	Average size \downarrow
baseline / ConfTS					
ResNet18	APS	0.90 / 0.90	14.1 (0.33) / 5.55 (0.23)	0.95 / 0.95	29.6 (1.08) / 17.8 (1.24)
	RAPS	0.90 / 0.90	5.21 (0.04) / 4.98 (0.16)	0.95 / 0.95	14.7 (0.46) / 12.6 (1.02)
ResNet50	APS	0.90 / 0.90	9.06 (0.36) / 2.92 (0.40)	0.95 / 0.95	20.0 (0.90) / 9.26 (0.95)
	RAPS	0.90 / 0.90	3.38 (0.05) / 2.56 (0.20)	0.95 / 0.95	9.21 (0.18) / 6.18 (0.76)
ResNet101	APS	0.90 / 0.90	6.95 (0.22) / 2.77 (0.70)	0.95 / 0.95	15.7 (1.06) / 7.81 (1.09)
	RAPS	0.90 / 0.90	2.90 (0.02) / 2.23 (0.14)	0.95 / 0.95	7.52 (0.17) / 5.52 (0.59)
Densenet121	APS	0.90 / 0.90	9.27 (0.28) / 5.87 (0.49)	0.95 / 0.95	20.3 (1.05) / 10.1 (1.00)
	RAPS	0.90 / 0.90	3.86 (0.06) / 2.88 (0.28)	0.95 / 0.95	12.3 (0.35) / 10.2 (0.54)
VGG16	APS	0.90 / 0.90	11.8 (0.36) / 4.58 (0.54)	0.95 / 0.95	23.7 (0.93) / 13.1 (1.21)
	RAPS	0.90 / 0.90	4.54 (0.06) / 3.87 (0.35)	0.95 / 0.95	12.3 (0.36) / 10.2 (0.55)
ViT	APS	0.90 / 0.90	14.6 (0.67) / 1.78 (0.18)	0.95 / 0.95	36.7 (1.91) / 6.19 (1.16)
	RAPS	0.90 / 0.90	2.84 (0.05) / 1.51 (0.02)	0.95 / 0.95	12.6 (0.78) / 3.63 (0.63)
Average	APS	0.90 / 0.90	10.9 / 3.91	0.95 / 0.95	24.3 / 10.71
	RAPS	0.90 / 0.90	3.79 / 3.01	0.95 / 0.95	11.44 / 8.06

(\mathbf{x}, y) , a threshold τ and the non-conformity score function $\mathcal{S}(\cdot)$, the compactness gap of the sample is given by:

$$\mathcal{G}(\mathbf{x}, y, \tau) = \tau - \mathcal{S}(\mathbf{x}, y)$$

In particular, a positive compactness gap $\mathcal{G} \in \mathbb{R}^+$ represents that the true label is included in the prediction set $y \in \mathcal{C}(\mathbf{x})$, and vice versa. In other words, we expect to increase the compactness gap for those examples with negative compactness gaps. Otherwise, we will decrease the compactness gap. As $\mathcal{S}(\mathbf{x}, y)$ is a function of the temperature t (See Eq. 9), we can optimize the compactness gap for satisfying the marginal coverage through the temperature value t .

Conformal Temperature Scaling. To this end, we propose *Conformal Temperature Scaling* (dubbed ConfTS), which rectifies the objective of temperature scaling through the compactness gap \mathcal{G} . In particular, the loss function is given by:

$$\ell(\mathbf{x}, y) = \begin{cases} \tau - \mathcal{S}(\mathbf{x}, y) & \mathbb{P}(\mathcal{G}(\mathbf{x}, y, \tau) > 0) \geq (1 - \alpha) \\ \mathcal{S}(\mathbf{x}, y) - \tau & \mathbb{P}(\mathcal{G}(\mathbf{x}, y, \tau) > 0) < (1 - \alpha) \end{cases}$$

where $\Pr(\mathcal{G}(\mathbf{x}, y, \tau) \geq 0)$ denotes the probability of the event that the compactness gap is positive. We omit the

temperature t for simplicity.

Following recent work (Stutz et al., 2022), the probability $\Pr(\mathcal{G}(\mathbf{x}, y, \tau) \geq 0)$ can be calculated as :

$$\mathbb{P}(\mathcal{G}(\mathbf{x}, y, \tau) \geq 0) = \phi(\tau - \mathcal{S}(\mathbf{x}, y)) \quad (10)$$

where $\phi(x) = 1/(1 + e^{-x})$ is the sigmoid function. Therefore, the loss function of ConfTS is defined as:

$$\ell(\mathbf{x}, y) = \text{sgn}(\phi(\tau - \mathcal{S}(\mathbf{x}, y)) - (1 - \alpha)) \cdot (\tau - \mathcal{S}(\mathbf{x}, y))$$

where $\text{sgn}(\cdot)$ denotes the sign function. The loss function is differentiable with respect to the temperature value, as both τ and $\mathcal{S}(\mathbf{x}, y)$ are functions of the temperature t .

During temperature scaling, we optimize the temperature t on the calibration set \mathcal{D}_{cal} , with the new loss function. Formally, the optimization can be formulated as:

$$t^* = \arg \min_{t \in \mathbb{R}^+} \mathbb{E}_{(\mathbf{x}, y) \in \mathcal{D}_{cal}} \ell(\mathbf{x}, y) \quad (11)$$

By way of conformal temperature scaling, the prediction set can be optimized to be compact while maintaining the property of marginal coverage.

5. Experiments

5.1. Experimental setup

Datasets. In this work, we use CIFAR100 (Krizhevsky et al., 2009), ImageNet (Deng et al., 2009) and ImageNet-V2 (Recht et al., 2019). Specifically, on ImageNet, we split the test dataset including 50000 images into 10000 images for the calibration set and 40000 images for the test set; on ImageNet-V2, we split the test dataset including 10000 images into 4000 images for the calibration set and 6000 for the test set. Additionally, we employ the same calibration set for determining the threshold τ and optimizing the temperature, aligning with the setting of model calibration in Conformal Prediction (Angelopoulos et al., 2021b).

Models. On ImageNet and ImageNet-V2, we employ six pre-trained classifiers on ImageNet: ResNet18, ResNet50, ResNet101 (He et al., 2016), DenseNet121 (Huang et al., 2017), VGG16 (Simonyan & Zisserman, 2015), ViT-B-16 (Dosovitskiy et al., 2021). On CIFAR100, we train these models from scratch.

Metric. We use *coverage* and *average size* defined in Section 2 to evaluate the performance of prediction sets. Additional results are provided in Appendix D.

5.2. Main results

Can ConfTS improve existing CP methods? In Table 2, we present the results of APS and RAPS with baseline and ConfTS respectively. A salient observation is that our method drastically improves APS performance by declining the average size of prediction sets. For example, for the ResNet50 model, when $\alpha = 0.1$, using ConfTS reduces the average size from 9.06 to 2.92 - a **6.14** of direct improvement; when $\alpha = 0.05$, our method decreases the average size from 29.7 to 17.9. Moreover, the results show that ConfTS can effectively reduce the average size of RAPS, while maintaining coverage rate. For example, for the ResNet50 model, when $\alpha = 0.1$ the baseline average size is 3.38, but reduces to 2.56 with ConfTS. Overall, the experiments show that our method not only benefits APS and RAPS but is effective on a diverse range of model architectures.

Does ConfTS work under distribution shifts? We also verify the effectiveness of our method on the new distribution, which is different from the training data distribution. Specifically, We divide the test dataset of ImageNet-V2, which exhibits a distribution shift compared to the ImageNet, equally into a calibration set containing 5000 images and a test set containing 5000 images. Then, the test models are only pre-trained on ImageNet and not be fine-tuned. Results in Table 3 show that our ConfTS can effectively improve APS and RAPS when the calibration set and test set come from a new distribution. For example, on ResNet18, ConfTS reduces the average size of APS from 31.47 to

Table 3. Performance comparison of conformal prediction with baseline and ConfTS under distribution shifts. We employ six models: ResNet18, ResNet50, ResNet101, DenseNet121, VGG16 and ViT pre-trained on ImageNet, and use ImageNet-V2 as the calibration set and test set. **Bold** numbers are superior results.

Model	Conformal	Coverage	Average size
		baseline / ConfTS	
ResNet18	APS	0.90 / 0.90	31.4 / 19.6
	RAPS	0.90 / 0.90	18.8 / 13.7
ResNet50	APS	0.90 / 0.90	24.6 / 11.9
	RAPS	0.90 / 0.90	13.3 / 11.3
ResNet101	APS	0.90 / 0.90	22.5 / 12.0
	RAPS	0.90 / 0.90	10.9 / 7.09
Densenet121	APS	0.90 / 0.90	50.3 / 13.3
	RAPS	0.90 / 0.90	13.7 / 9.63
VGG16	APS	0.90 / 0.90	27.2 / 17.9
	RAPS	0.90 / 0.90	16.3 / 12.6
ViT	APS	0.90 / 0.90	34.2 / 10.1
	RAPS	0.90 / 0.90	14.9 / 4.62

19.69, and decreases that of RAPS from 18.87 to 13.73. In conclusion, the results demonstrate that our method can improve APS and RAPS under distribution shifts.

ConfTS vs. Entropy Minimization. In Section 3.2, we show that a confident prediction often leads to a compact prediction set. We note that entropy minimization is a common practice to increase the confidence of prediction (Grandvalet & Bengio, 2004). In this part, we show that directly applying entropy minimization does not work better than ConfTS. Specifically, we consider the alternative loss function:

$$\mathcal{L}_{entropy}(\mathbf{x}, y) = -\log \pi_y(\mathbf{x}) + \gamma \mathcal{H}(\pi(\mathbf{x}))$$

where $\mathcal{H}(\cdot)$ is the entropy of the softmax probability distribution. Here, we conduct experiments with the ResNet50 model on ImageNet using APS and $\alpha = 0.1$.

The results in Table 4 show that both ConfTS and entropy minimization could reduce average set size while maintaining the desired coverage rate. However, the entropy minimization suffers from optimization difficulty and occasionally falls short of enhancing APS when γ is too large. In addition, our method does not require hyperparameter tuning, while the entropy minimization needs to search for a proper γ . Overall, we show that simply boosting the probability entropy may hurt the prediction set while ConfTS significantly improves the performance.

ConfTS maintains adaptiveness. Adaptiveness, as a common desideratum for conformal prediction, requires prediction sets to communicate instance-wise uncertainty: they

Table 4. Coverage rate and average set size of APS for ConfTS and entropy minimization, using a pre-trained ResNet50 model on ImageNet. “T” represents the optimal temperature. **Bold** numbers are the optimal result.

Loss	T	coverage	average size
ConfTS(our)	0.54	0.90	5.55
Entropy minimization	$\gamma = 0.5$	1.11	5.66
	$\gamma = 0.2$	0.87	7.91
	$\gamma = 0.1$	0.62	9.47

should be smaller for easy test-time examples than for hard ones (Seedat et al., 2023). In this part, we examine the impact of ConfTS on the adaptability of prediction sets. We use the label order $o(y, \pi(\mathbf{x}))$ to present instance difficulty, and compare the performance of prediction sets for samples of different difficulties. Specifically, we partition the sample by label order: 1, 2-3, 4-6, 7-10, 11-100, 101-1000. We use the ResNet50 model on the ImageNet and employ APS and RAPS with $\alpha = 0.1$.

Figure 3 demonstrates that the prediction sets produced by APS and RAPS with ConfTS maintain adaptiveness. Specifically, our method provides smaller prediction sets for easy samples than those of hard examples. Overall, the results highlight the advantage of ConfTS in improving the prediction set adaptively.

6. Related Work

Conformal Prediction. Conformal prediction (Vovk et al., 2005; Papadopoulos et al., 2002) is a promising framework for uncertainty qualification. Many prior works applied conformal prediction in various settings, including regression (Lei & Wasserman, 2014; Romano et al., 2019), classification (Sadinle et al., 2019), object detection (Angelopoulos et al., 2021a), outlier detection (Liang et al., 2022; Guan & Tibshirani, 2022; Bates et al., 2023), Large-Language Model (Kumar et al., 2023; Ren et al., 2023).

1) Some methods aim to generate a compact prediction set, such as developing new training algorithms (Colombo & Vovk, 2020; Chen et al., 2021). The other avenue involves leveraging post-hoc technologies (Romano et al., 2020; Ghosh et al., 2023), and most existing post-hoc methods leverage temperature scaling for better calibration performance (Angelopoulos et al., 2021b; Lu et al., 2022; 2023; Gibbs et al., 2023). In our work, we first show that post-hoc calibration methods increase the size of the prediction set, which motivates us to design a novel post-hoc logits rescaling method to encourage compact prediction sets.

2) Some methods seek to enhance the coverage rate, including efforts to maintain the marginal coverage rate by modi-

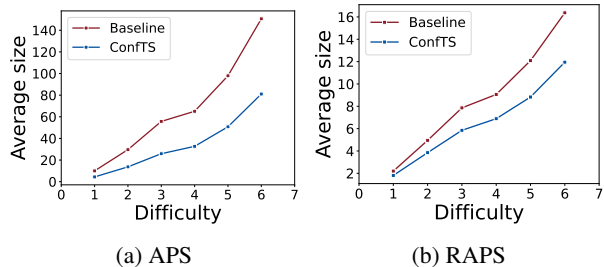


Figure 3. Average set size vs. difficulty. We report the average size using the ResNet50 model pre-trained on ImageNet. The “Difficulty” is the ranking of the true class’s estimated probability.

fying the assumption of exchangeability such as adversaries (Gendler et al., 2021), covariate shifts (Tibshirani et al., 2019), label shifts (Podkopaev & Ramdas, 2021). Moreover, a line of works seeks to construct adaptive sets or intervals (Romano et al., 2020; Seedat et al., 2023; Angelopoulos et al., 2021b) to communicate instance uncertainty. In this work, we demonstrate that our ConfTS could maintain the adaptiveness of existing CP methods.

Calibration. Confidence calibration has been studied in various contexts in recent years. Some works address the miscalibration problem by post-hoc methods like histogram binning (Zadrozny & Elkan, 2001), isotonic regression (Zadrozny & Elkan, 2002), and Platt scaling (Platt et al., 1999). Besides, regularization methods like entropy regularization (Pereyra et al., 2017) and focal loss (Mukhoti et al., 2020) are also proposed to improve the calibration quality of deep neural networks.

7. Conclusion

In this paper, we first show that post-hoc calibration methods can lead to larger prediction sets, while over-confidence (with temperature $t < 1$) can surprisingly decrease the average size. We theoretically show that predictions with high confidence increase the non-conformity score, thereby resulting in a lower probability of appending a new class in the prediction set. Inspired by this analysis, we propose Conformal Temperature Scaling (ConfTS), a small modification to Temperature Scaling. Specifically, we design a novel loss function that reflects how a prediction set distances from the optimal set, and we substitute this loss function for the cross-entropy loss in temperature scaling. Experiments show that our ConfTS can not only effectively improve APS and RAPS, while maintaining computational efficiency but also preserve the adaptiveness of prediction sets. In summary, this work uncovers the relationship between calibration and conformal prediction, which provides a guideline for future work to use confidence calibration properly and may inspire specifically designed methods.

Impact Statements

This paper presents work whose goal is to advance the field of Machine Learning. There are many potential societal consequences of our work, none of which we feel must be specifically highlighted here.

References

- Angelopoulos, A. N. and Bates, S. A gentle introduction to conformal prediction and distribution-free uncertainty quantification. *arXiv preprint arXiv:2107.07511*, 2021.
- Angelopoulos, A. N., Bates, S., Candès, E. J., Jordan, M. I., and Lei, L. Learn then test: Calibrating predictive algorithms to achieve risk control. *arXiv preprint arXiv:2110.01052*, 2021a.
- Angelopoulos, A. N., Bates, S., Jordan, M. I., and Malik, J. Uncertainty sets for image classifiers using conformal prediction. In *9th International Conference on Learning Representations, ICLR 2021, Virtual Event, Austria, May 3-7, 2021*. OpenReview.net, 2021b.
- Balasubramanian, V., Ho, S.-S., and Vovk, V. *Conformal prediction for reliable machine learning: theory, adaptations and applications*. Newnes, 2014.
- Bates, S., Candès, E., Lei, L., Romano, Y., and Sesia, M. Testing for outliers with conformal p-values. *The Annals of Statistics*, 51(1):149–178, 2023.
- Chen, H., Huang, Z., Lam, H., Qian, H., and Zhang, H. Learning prediction intervals for regression: Generalization and calibration. In *International Conference on Artificial Intelligence and Statistics*, pp. 820–828. PMLR, 2021.
- Colombo, N. and Vovk, V. Training conformal predictors. In *Conformal and Probabilistic Prediction and Applications*, pp. 55–64. PMLR, 2020.
- Deng, J., Dong, W., Socher, R., Li, L.-J., Li, K., and Fei-Fei, L. Imagenet: A large-scale hierarchical image database. In *2009 IEEE conference on Computer Vision and Pattern Recognition*, pp. 248–255. Ieee, 2009.
- Dosovitskiy, A., Beyer, L., Kolesnikov, A., Weissenborn, D., Zhai, X., Unterthiner, T., Dehghani, M., Minderer, M., Heigold, G., Gelly, S., Uszkoreit, J., and Houlsby, N. An image is worth 16x16 words: Transformers for image recognition at scale. In *9th International Conference on Learning Representations, ICLR 2021, Virtual Event, Austria, May 3-7, 2021*. OpenReview.net, 2021.
- Gal, Y. and Ghahramani, Z. Dropout as a bayesian approximation: Representing model uncertainty in deep learning. In *International Conference on Machine Learning*, pp. 1050–1059. PMLR, 2016.
- Gendler, A., Weng, T.-W., Daniel, L., and Romano, Y. Adversarially robust conformal prediction. In *International Conference on Learning Representations*, 2021.
- Ghosh, S., Belkhouja, T., Yan, Y., and Doppa, J. R. Improving uncertainty quantification of deep classifiers via neighborhood conformal prediction: Novel algorithm and theoretical analysis. *arXiv preprint arXiv:2303.10694*, 2023.
- Gibbs, I., Cherian, J. J., and Candès, E. J. Conformal prediction with conditional guarantees. *arXiv preprint arXiv:2305.12616*, 2023.
- Grandvalet, Y. and Bengio, Y. Semi-supervised learning by entropy minimization. *Advances in Neural Information Processing Systems*, 17, 2004.
- Guan, L. and Tibshirani, R. Prediction and outlier detection in classification problems. *Journal of the Royal Statistical Society Series B: Statistical Methodology*, 84(2):524–546, 2022.
- Guo, C., Pleiss, G., Sun, Y., and Weinberger, K. Q. On calibration of modern neural networks. In *International Conference on Machine Learning*, pp. 1321–1330. PMLR, 2017.
- He, K., Zhang, X., Ren, S., and Sun, J. Deep residual learning for image recognition. In *Proceedings of the IEEE Conference on Computer Vision and Pattern Recognition*, pp. 770–778, 2016.
- Huang, G., Liu, Z., Van Der Maaten, L., and Weinberger, K. Q. Densely connected convolutional networks. In *Proceedings of the IEEE conference on Computer Vision and Pattern Recognition*, pp. 4700–4708, 2017.
- Krizhevsky, A., Hinton, G., et al. Learning multiple layers of features from tiny images. 2009.
- Kumar, B., Lu, C., Gupta, G., Palepu, A., Bellamy, D. R., Raskar, R., and Beam, A. Conformal prediction with large language models for multi-choice question answering. *CoRR*, abs/2305.18404, 2023. doi: 10.48550/ARXIV.2305.18404.
- Lei, J. Classification with confidence. *Biometrika*, 101(4): 755–769, 2014.
- Lei, J. and Wasserman, L. Distribution-free prediction bands for non-parametric regression. *Journal of the Royal Statistical Society Series B: Statistical Methodology*, 76(1): 71–96, 2014.
- Liang, Z., Sesia, M., and Sun, W. Integrative conformal p-values for powerful out-of-distribution testing with labeled outliers. *arXiv preprint arXiv:2208.11111*, 2022.

- Lu, C., Ahmed, S. R., Singh, P., and Kalpathy-Cramer, J. Estimating test performance for AI medical devices under distribution shift with conformal prediction. *CoRR*, abs/2207.05796, 2022. doi: 10.48550/ARXIV.2207.05796.
- Lu, C., Yu, Y., Karimireddy, S. P., Jordan, M., and Raskar, R. Federated conformal predictors for distributed uncertainty quantification. In *International Conference on Machine Learning*, pp. 22942–22964. PMLR, 2023.
- Mukhoti, J., Kulharia, V., Sanyal, A., Golodetz, S., Torr, P., and Dokania, P. Calibrating deep neural networks using focal loss. *Advances in Neural Information Processing Systems*, 33:15288–15299, 2020.
- Müller, R., Kornblith, S., and Hinton, G. E. When does label smoothing help? *Advances in Neural Information Processing Systems*, 32, 2019.
- Papadopoulos, H., Proedrou, K., Vovk, V., and Gammerman, A. Inductive confidence machines for regression. In *Machine Learning: ECML 2002: 13th European Conference on Machine Learning Helsinki, Finland, August 19–23, 2002 Proceedings 13*, pp. 345–356. Springer, 2002.
- Pereyra, G., Tucker, G., Chorowski, J., Kaiser, L., and Hinton, G. E. Regularizing neural networks by penalizing confident output distributions. In *5th International Conference on Learning Representations, ICLR 2017, Toulon, France, April 24–26, 2017, Workshop Track Proceedings*. OpenReview.net, 2017.
- Platt, J. et al. Probabilistic outputs for support vector machines and comparisons to regularized likelihood methods. *Advances in Large Margin Classifiers*, 10(3):61–74, 1999.
- Podkopaev, A. and Ramdas, A. Distribution-free uncertainty quantification for classification under label shift. In *Uncertainty in Artificial Intelligence*, pp. 844–853. PMLR, 2021.
- Recht, B., Roelofs, R., Schmidt, L., and Shankar, V. Do imagenet classifiers generalize to imagenet? In *International Conference on Machine Learning*, pp. 5389–5400. PMLR, 2019.
- Ren, A. Z., Dixit, A., Bodrova, A., Singh, S., Tu, S., Brown, N., Xu, P., Takayama, L., Xia, F., Varley, J., et al. Robots that ask for help: Uncertainty alignment for large language model planners. In *7th Annual Conference on Robot Learning*, 2023.
- Romano, Y., Patterson, E., and Candes, E. Conformalized quantile regression. *Advances in Neural Information Processing Systems*, 32, 2019.
- Romano, Y., Sesia, M., and Candes, E. Classification with valid and adaptive coverage. *Advances in Neural Information Processing Systems*, 33:3581–3591, 2020.
- Sadinle, M., Lei, J., and Wasserman, L. Least ambiguous set-valued classifiers with bounded error levels. *Journal of the American Statistical Association*, 114(525):223–234, 2019.
- Seedat, N., Jeffares, A., Imrie, F., and van der Schaar, M. Improving adaptive conformal prediction using self-supervised learning. In *International Conference on Artificial Intelligence and Statistics*, pp. 10160–10177. PMLR, 2023.
- Shafer, G. and Vovk, V. A tutorial on conformal prediction. *Journal of Machine Learning Research*, 9(3), 2008.
- Simonyan, K. and Zisserman, A. Very deep convolutional networks for large-scale image recognition. In Bengio, Y. and LeCun, Y. (eds.), *3rd International Conference on Learning Representations, ICLR 2015, San Diego, CA, USA, May 7–9, 2015, Conference Track Proceedings*, 2015.
- Smith, R. C. *Uncertainty quantification: theory, implementation, and applications*, volume 12. Siam, 2013.
- Stutz, D., Dvijotham, K., Cemgil, A. T., and Doucet, A. Learning optimal conformal classifiers. In *The Tenth International Conference on Learning Representations, ICLR 2022, Virtual Event, April 25–29, 2022*. OpenReview.net, 2022.
- Tibshirani, R. J., Foygel Barber, R., Candes, E., and Ramdas, A. Conformal prediction under covariate shift. *Advances in Neural Information Processing Systems*, 32, 2019.
- Vovk, V., Gammerman, A., and Saunders, C. Machine-learning applications of algorithmic randomness. 1999.
- Vovk, V., Gammerman, A., and Shafer, G. *Algorithmic learning in a random world*, volume 29. Springer, 2005.
- Wang, C. Calibration in deep learning: A survey of the state-of-the-art. *arXiv preprint arXiv:2308.01222*, 2023.
- Wang, D.-B., Feng, L., and Zhang, M.-L. Rethinking calibration of deep neural networks: Do not be afraid of overconfidence. *Advances in Neural Information Processing Systems*, 34:11809–11820, 2021.
- Wei, H., Xie, R., Cheng, H., Feng, L., An, B., and Li, Y. Mitigating neural network overconfidence with logit normalization. In *International Conference on Machine Learning*, pp. 23631–23644. PMLR, 2022.

Yuksekgonul, M., Zhang, L., Zou, J., and Guestrin, C. Beyond confidence: Reliable models should also consider atypicality. In *Thirty-seventh Conference on Neural Information Processing Systems*, 2023.

Zadrozny, B. and Elkan, C. Obtaining calibrated probability estimates from decision trees and naive bayesian classifiers. In *International Conference on Machine Learning*, volume 1, pp. 609–616, 2001.

Zadrozny, B. and Elkan, C. Transforming classifier scores into accurate multiclass probability estimates. In *Proceedings of the eighth ACM SIGKDD International Conference on Knowledge Discovery and Data mining*, pp. 694–699, 2002.

A. Post-hoc Calibration Methods

Here, we briefly review three calibration methods, whose parameters are optimized with respect to NLL on the calibration set.

Platt Scaling (Platt et al., 1999) is a parametric approach to calibration. Let \mathbf{f} be an arbitrary logits vector. Platt Scaling learns scalar parameters $a, b \in \mathcal{R}$ and outputs

$$\pi = \sigma(a\mathbf{f} + b) \tag{12}$$

Temperature Scaling (Guo et al., 2017) was inspired by (Platt et al., 1999), using a scalar parameter t for all logits vectors. Formally, for any given logits vector \mathbf{f} , the new predicted logits is

$$\pi = \sigma(\mathbf{f}/t)$$

Intuitively, t softens the softmax logits when $t > 1$ so that it alleviates over-confidence.

Vector Scaling (Guo et al., 2017) is a simple extension of Platt scaling. Let \mathbf{f} be an arbitrary logit vector, which is produced before the softmax layer. Vector scaling applies a linear transformation to the given vector:

$$\pi = \sigma(M\mathbf{f} + b)$$

where $M \in \mathbb{R}^{K \times K}$ is a diagonal matrix and $b \in \mathbb{R}^K$.

A.1. Why do Platt scaling and temperature scaling maintain label order but vector fails?

Theorem A.1. For any given logits (f_1, \dots, f_K) , where $f_1 > f_2 > \dots > f_K$, if $a > 0, b \in \mathbb{R}$, we have

$$\frac{e^{af_i+b}}{\sum_{k=1}^K e^{af_k+b}} > \frac{e^{af_j+b}}{\sum_{k=1}^K e^{af_k+b}}$$

where $i > j$.

Proof. $e^{af_i+b} = e^{af_i}e^b > e^{af_j}e^b = e^{af_j+b}$ □

Remark A.2. From Proposition A.1, we find that Platt scaling does not change the order of prediction probabilities. Moreover, temperature scaling is a simple version of vector scaling, i.e., $b = 0$. Thus, temperature scaling also maintains the prediction order.

The above two theorems show that each label maintains its order with temperature scaling and Platt scaling. For vector scaling, we consider a binary classification problem, where the original logits vector is $f = (f_1, f_2)^T$. We define a vector scaling function:

$$V(f) = \begin{pmatrix} 1 & 0 \\ 0 & 100 \end{pmatrix} \times f = \begin{pmatrix} f_1 \\ 101 \times f_2 \end{pmatrix}.$$

Let f be $(100, 1)^T$ whose predicted class \hat{y} is 1. After vector scaling, $V(f) = (100, 101)^T$ whose predicted class \hat{y} is 2, indicating label order has changed.

B. Experiment Setup

We use two datasets in our study: ImageNet (Deng et al., 2009) and CIFAR-100 (Krizhevsky et al., 2009). We employ six classifiers: ResNet50, ResNet18, ResNet101, DenseNet121, VGG16. On ImageNet, we simply use pre-trained models on Pytorch. On CIFAR-100, we train these models from scratch. In the case of ImageNet, we split the test dataset containing 50000 images into 30000 images for the calibration set and 20000 images for the test set. For CIFAR-100, We divide the corresponding test dataset equally into a calibration set containing 5000 images and a test set containing 5000 images. We set $\alpha = 0.1$. When we use RAPS to generate prediction sets, the hyperparameters are set to be $k_{reg} = 1$ and $\lambda = 0.001$.

C. How does model calibration affect the coverage rate of prediction sets?

We compare the coverage rate of prediction sets with and without calibration methods. Results show that Platt scaling and temperature scaling exhibit negligible impact on coverage rate, while vector scaling may hurt coverage rate. For example, on ImageNet, the original coverage rate of ResNet18 is 0.9, and remains unchanged with Platt scaling and temperature scaling, but reduces to 0.88 with vector scaling. This difference may stem from the fact that Platt scaling and temperature scaling maintain the label order in the probability output, while vector scaling alters it. Rigorous proofs are available in Appendix A.1. Consequently, minor adjustments to softmax probability $\pi(\mathbf{x})$ do not significantly affect the exchangeability of samples, thereby holding the error rate of prediction sets (see Theorem 2.1). This finding suggests the potential to enhance conformal prediction by using post-hoc method to slightly modify the posterior probability.

D. Additional experimental results

D.1. Additional results of Section 3.1

In this section, we report more results of how prediction sets perform with calibration methods. We can see after being employed with calibration methods, models tend to generate larger prediction sets, which indicate higher uncertainty.

Table 5. Results on CIFAR-100 and ImageNet for various models and different calibration methods: baseline (BS), vector scaling (VS), Platt scaling (PS), and temperature scaling (TS). ▼ indicates smaller values are better.

Datasets	Metrics	DenseNet				VGG16				Inception				
		BS	VS	PS	TS	BS	VS	PS	TS	BS	VS	PS	TS	
CIFAR-100	Accuracy	0.70	0.72	0.70	0.70	0.72	0.72	0.72	0.72	0.80	0.80	0.80	0.80	
	APS	Coverage	0.90	0.89	0.90	0.90	0.90	0.89	0.90	0.90	0.90	0.89	0.90	0.90
		Average size ▼	5.22	4.89	7.14	7.52	4.41	5.31	5.94	6.04	10.6	10.2	11.6	11.7
	RAPS	Coverage	0.90	0.89	0.90	0.90	0.90	0.89	0.90	0.90	0.90	0.89	0.90	0.90
		Average size ▼	3.24	3.28	4.38	4.65	4.46	3.80	4.19	4.32	4.92	4.08	4.41	4.62
	ImageNet	Accuracy	0.74	0.73	0.74	0.74	0.72	0.70	0.72	0.72	0.69	0.69	0.69	0.69
APS		Coverage	0.90	0.89	0.90	0.90	0.90	0.88	0.90	0.90	0.90	0.88	0.90	0.90
		Average size ▼	9.85	6.09	11.9	8.57	11.4	6.38	13.6	11.6	38.2	43.2	95.7	93.7
RAPS		Coverage	0.90	0.89	0.90	0.90	0.90	0.88	0.90	0.90	0.90	0.88	0.90	0.90
		Average size ▼	3.87	3.05	4.35	3.59	4.47	3.33	4.99	4.51	5.11	5.11	8.49	8.30

D.2. Additional results of Section 3.2

In this section, we offer additional results of how a confident prediction influences prediction sets. We can observe that high confidence often results in smaller and more informative prediction sets.

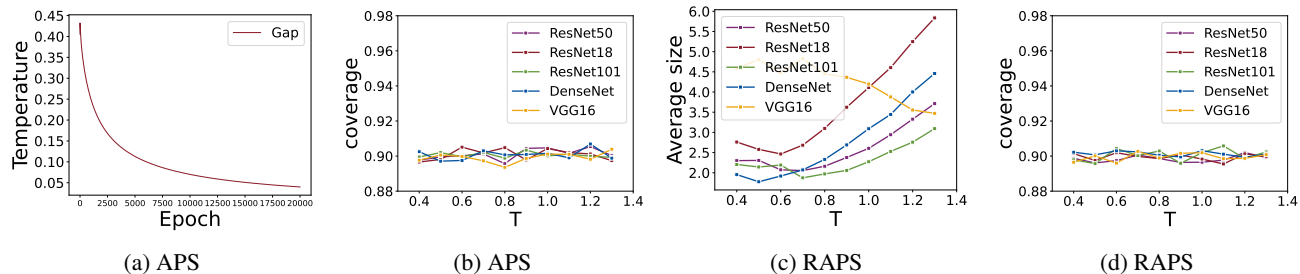


Figure 4. Results on CIFAR-100. We report the average size and coverage rate of APS and RAPS using five models with different temperatures.

Does Confidence Calibration Help Conformal Prediction?

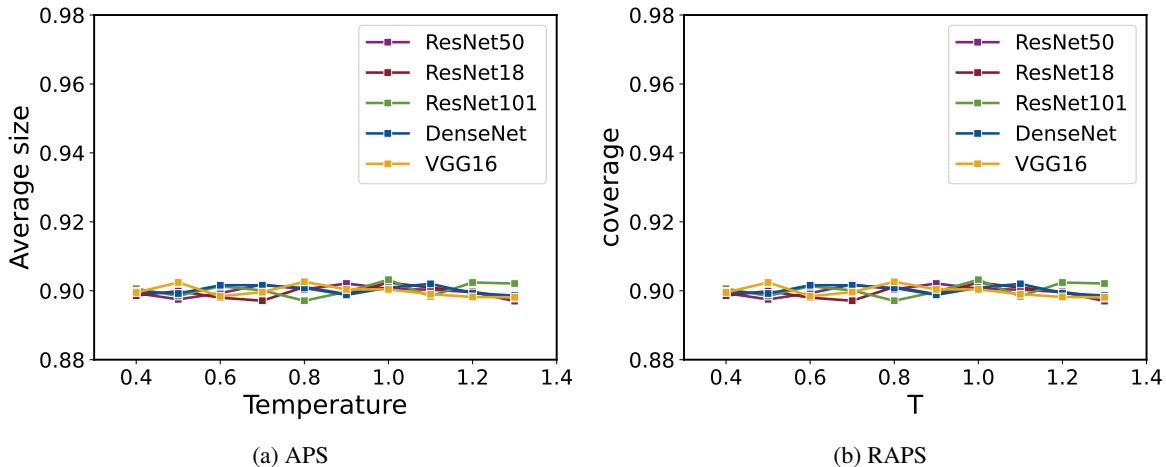


Figure 5. Coverage rate for various models on different temperatures. We report the average size of APS and RAPS using five models pre-trained on ImageNet.

D.3. Additional results of Section 5

In this section, we show our method ConfTTS can effectively improve conformal prediction. Results show that after being employed with ConfTTS, models tend to construct smaller prediction sets but maintain the desired coverage rate.

Table 6. Performance comparison of different non-conformity scores with or without ConfTTS. We employ six models pre-trained on ImageNet. The calibration set and test set are from ImageNet-v2. ↓ indicates smaller values are better.

Model	Conformal	alpha=0.1		alpha=0.05	
		Coverage	Average size ↓	Coverage	Average size ↓
baseline / ConfTTS					
ResNet18	APS	0.9/0.9	31.47 / 19.69	0.95/0.95	71.21 / 58.56
	RAPS	0.9/0.9	18.87 / 13.73	0.95/0.95	30.57 / 44.90
ResNet50	APS	0.9/0.9	24.64 / 11.90	0.95/0.95	53.32 / 43.09
	RAPS	0.9/0.9	13.36 / 11.37	0.95/0.95	20.57 / 23.61
ResNet101	APS	0.9/0.9	22.59 / 12.00	0.95/0.95	48.06 / 39.47
	RAPS	0.9/0.9	10.98 / 7.09	0.95/0.95	16.66 / 22.24
Densenet121	APS	0.9/0.9	50.39 / 13.30	0.95/0.95	50.38 / 40.73
	RAPS	0.9/0.9	13.71 / 9.63	0.95/0.95	21.33 / 33.65
VGG16	APS	0.9/0.9	27.25 / 17.91	0.95/0.95	60.85 / 48.88
	RAPS	0.9/0.9	16.32 / 12.61	0.95/0.95	25.33 / 37.92
ViT	APS	0.9/0.9	34.21 / 10.17	0.95/0.95	87.89 / 62.28
	RAPS	0.9/0.9	14.99 / 4.62	0.95/0.95	29.69 / 16.25

Table 7. Performance comparison of different non-conformity scores with or without ConfTS. We employ five models trained on CIFAR100. ↓ indicates smaller values are better.

Model	Conformal	alpha=0.1		alpha=0.05	
		Coverage	Average size	Coverage	Average size
baseline / ConfTS					
ResNet18	APS	0.9/0.9	8.73 / 3.79	0.95/0.95	15.7 / 11.7
	RAPS	0.9/0.9	7.16 / 2.56	0.95/0.95	11.3 / 6.54
ResNet50	APS	0.9/0.9	4.91 / 2.80	0.95/0.95	10.1 / 7.81
	RAPS	0.9/0.9	4.01 / 2.06	0.95/0.95	6.71 / 5.16
ResNet101	APS	0.9/0.9	4.01 / 2.30	0.95/0.95	8.61 / 7.09
	RAPS	0.9/0.9	3.37 / 1.88	0.95/0.95	5.25 / 4.84
Densenet121	APS	0.9/0.9	5.98 / 2.34	0.95/0.95	11.7 / 6.64
	RAPS	0.9/0.9	5.06 / 1.78	0.95/0.95	8.03 / 4.35
VGG16	APS	0.9/0.9	4.56 / 4.31	0.95/0.95	10.4 / 10.5
	RAPS	0.9/0.9	3.56 / 4.21	0.95/0.95	11.3 / 11.4

E. Omitted Proof

E.1. Proof for Proposition 3.1

Lemma E.1. For any given logits (f_1, \dots, f_n) , where $f_1 > f_2 > \dots > f_n$, and constant $t > 1$, we have

$$\frac{e^{tf_n}}{\sum_{i=1}^n e^{tf_i}} < \frac{e^{f_n}}{\sum_{i=1}^n e^{f_i}}$$

Proof. Let $t = 1 + s$. Then, we have

$$\begin{aligned} \frac{e^{tf_n}}{\sum_{i=1}^n e^{tf_i}} &= \frac{e^{(1+s)f_n}}{\sum_{i=1}^n e^{(1+s)f_i}} \\ &= \frac{e^{f_n}}{\sum_{i=1}^n e^{f_i} e^{s(f_i - f_n)}} \\ &< \frac{e^{f_1}}{\sum_{i=1}^n e^{f_i}} \end{aligned}$$

□

Lemma E.2. For any given logits (f_1, \dots, f_K) , where $f_1 > f_2 > \dots > f_K$, and constant $t > 1$, we have

$$\sum_{i=1}^k \frac{e^{tf_i}}{\sum_{j=1}^K e^{tf_j}} \geq \sum_{i=1}^k \frac{e^{f_i}}{\sum_{j=1}^K e^{f_j}}, \forall k = 1, \dots, K$$

The equation holds if and only if $k = K$.

Proof. By Lemma E.1, we have

$$\frac{e^{tf_n}}{\sum_{i=1}^n e^{tf_i}} < \frac{e^{f_n}}{\sum_{i=1}^n e^{f_i}}$$

Since

$$\sum_{i=1}^n \frac{e^{tf_i}}{\sum_{j=1}^n e^{tf_j}} = \sum_{i=1}^n \frac{e^{f_i}}{\sum_{j=1}^n e^{f_j}} = 1$$

we can get

$$\sum_{i=1}^{n-1} \frac{e^{tf_i}}{\sum_{j=1}^n e^{tf_j}} > \sum_{i=1}^{n-1} \frac{e^{f_i}}{\sum_{j=1}^n e^{f_j}}$$

Assume that

$$\sum_{i=1}^{n-2} \frac{e^{tf_i}}{\sum_{j=1}^n e^{tf_j}} < \sum_{i=1}^{n-2} \frac{e^{f_i}}{\sum_{j=1}^n e^{f_j}}$$

which indicates

$$\frac{e^{tf_{n-1}}}{\sum_{i=1}^n e^{tf_i}} > \frac{e^{f_{n-1}}}{\sum_{i=1}^n e^{f_i}}$$

From Lemma E.1, we know for $\forall k = 1, 2, \dots, n-2$,

$$\frac{e^{tf_k}}{\sum_{i=1}^n e^{tf_i}} > \frac{e^{f_k}}{\sum_{i=1}^n e^{f_i}}$$

Thus,

$$\sum_{i=1}^{n-2} \frac{e^{tf_i}}{\sum_{j=1}^n e^{tf_j}} > \sum_{i=1}^{n-2} \frac{e^{f_i}}{\sum_{j=1}^n e^{f_j}}$$

where we get a contradiction. Therefore, by induction, we can get

$$\sum_{i=1}^k \frac{e^{tf_i}}{\sum_{j=1}^n e^{tf_j}} \geq \sum_{i=1}^k \frac{e^{f_i}}{\sum_{j=1}^n e^{f_j}}, \forall k = 1, \dots, n$$

where the equation holds if and only if $k = n$. □

Proposition E.3 (restatement of Proposition 3.1). *For any data sample (\mathbf{x}, y) , let $\mathcal{S}(\mathbf{x}, y, t)$ denote the non-conformity scores. If $t_1 \geq t_2$, we have*

$$\mathcal{S}(\mathbf{x}, y, t_1) \leq \mathcal{S}(\mathbf{x}, y, t_2)$$

Proof. Directly hold from Lemma E.2. □

E.2. Proof for Theorem 3.2

Lemma E.4. *If the model \hat{f} is well-calibrated, i.e.,*

$$\pi_y(X) = \hat{f}(X)_y = P\{Y = y|X\}, \forall y$$

then the non-conformity score is uniformly distributed conditional on X , that is

$$P\{s < \alpha|X\} = \alpha, \forall \alpha \in [0, 1]$$

Proof. For any given sample (X, y) , suppose we want to construct prediction set $\mathcal{C}(X)$ with any given error rate $\alpha \in [0, 1]$. Without loss of generality, let $\pi_1(X) > \pi_2(X) > \dots > \pi_K(X)$ and the true label y be in j^{th} place. Thus, we know

$$s = \mathcal{S}(X, y) = \pi_1(X) + \pi_2(X) + \dots + \pi_j(X)$$

Since the model is well-calibrated, the desired set is

$$\mathcal{C}(X) = \{\text{smallest } \{1, 2, \dots, k\} : \pi_1(X) + \pi_2(X) + \dots + \pi_k(X) \geq 1 - \alpha\}$$

Then,

$$\begin{aligned} P\{s < 1 - \alpha | X\} &= P\{\mathcal{S}(X) < 1 - \alpha\} \\ &= P\{y \in \mathcal{C}(X)\} \\ &= 1 - \alpha \end{aligned}$$

which is equal to

$$P\{s < \alpha | X\} = \alpha$$

□

The following proof is essentially based on (Lei, 2014; Sadinle et al., 2019).

Theorem E.5 (restatement of Theorem 3.2). *Suppose the model is well-calibrated defined in 12. For any data sample \mathbf{x} , let its non-conformity score be $\mathcal{S}(\mathbf{x}, y)$ and threshold be τ ; after applying temperature $t < 1$, let its non-conformity score be $\mathcal{S}'(\mathbf{x}, y)$ and threshold be τ' . Let $G_y(\cdot)$ denote the cdf of $\mathcal{S}(\mathbf{x}, y)$. Give the assumption that*

$$\begin{aligned} (a) & P\{\sup_x \{\mathcal{S}'(\mathbf{x}, y) - \mathcal{S}(\mathbf{x}, y)\} \leq \epsilon\} \leq \delta \\ (b) & \exists \gamma, c_1, c_2, \epsilon_0, \forall \epsilon \in [-\epsilon_0, \epsilon_0] \quad s.t. c_1 |\epsilon|^\gamma \leq |G_y(t + \epsilon) - G_y(t)| \leq c_2 |\epsilon|^\gamma \end{aligned}$$

Then, there exists a constant c such that with probability $1 - M\delta - n^{-1}$:

$$P\{y \in \mathcal{C}/\mathcal{C}'\} \geq 2\epsilon + \{(M + 1)cc_1^{-1}(\log n/n)\}^{1/\gamma}$$

Proof. Let $G'_y(\cdot)$ be the empirical distribution of $\mathcal{S}(\mathbf{x}_i, y)$, for $i \in \mathcal{I}_{cal}$. Let $\hat{P}(\cdot)$ be the probability measure corresponding to $G'_y(\cdot)$. Define $C_y(s) = \{\mathbf{x} : \mathcal{S}(\mathbf{x}, y) < s\}$, $C'_y(s) = \{\mathbf{x} : \mathcal{S}'(\mathbf{x}, y) < s'\}$. We consider the event:

$$\begin{aligned} E = & \{\sup_x \{\mathcal{S}'(\mathbf{x}, y) - \mathcal{S}(\mathbf{x}, y)\} \geq \epsilon, \\ & \sup_{y, s} |G'_y - G_y(t)| \leq c(\log n/n)^{1/2}, \\ & \sup_y |P'\{Y = y\} - P\{Y = y\}| \leq c(\log n/n)^{1/2}\} \end{aligned}$$

which has probability at least $1 - M\delta - n^{-1}$ if c is chosen large enough and M grows slowly with n . Let \hat{P} be the empirical probability distribution that assigns probability $1/n_1$ to $X_{1,i}$, $\forall i = 1, 2, \dots, n_1$. We have

$$\begin{aligned} \hat{P}(C'_y(s)) &\leq \hat{P}(C_y(x + \epsilon)) \\ &= G'_y(s + \epsilon) \\ &\leq G_y(s + \epsilon) + c(\log n/n)^{1/2} \end{aligned}$$

Let $s^* = s - \epsilon - [(M + 1)cc_1^{-1}(\log n/n)^{1/2}]^{1/\gamma}$. Then,

$$\begin{aligned} \hat{P}(C'_y(s^*)) &\leq G_y(s - [(M + 1)cc_1^{-1}(\log n/n)^{1/2}]^{1/\gamma}) \\ &\quad + c(\log n/n)^{1/2} \\ &\leq G_y(s) - cM(\log n/n)^{1/2} \\ &\leq \hat{P}(C'_y(s')) \end{aligned}$$

Therefore,

$$s' \geq s^* = s - \epsilon - [(M + 1)cc_1^{-1}(\log n/n)^{1/2}]^{1/\gamma}$$

It follows that

$$\begin{aligned} P\{y \in \mathcal{C}/\mathcal{C}'\} &= P\{S(\mathbf{x}, y) < s, S'(\mathbf{x}, y) \geq s'\} \\ &\geq P\{s > S(X, y) \geq s' - \epsilon\} \\ &\geq P\{s > S(X, y) \geq s - 2\epsilon - \\ &\quad [(M + 1)cc_1^{-1}(\log n/n)^{1/2}]^{1/\gamma}\} \end{aligned}$$

From Lemma E.4, we have

$$P\{y \in \mathcal{C}/\mathcal{C}'\} = 2\epsilon + [(M + 1)cc_1^{-1}(\log n/n)^{1/2}]^{1/\gamma}$$

□